© 2023. Published by The Company of Biologists Ltd | Development (2023) 150, dev200879. doi:10.1242/dev.200879

STEM CELLS AND REGENERATION

RESEARCH ARTICLE

Developmental trajectory of pluripotent stem cell establishment in *Arabidopsis* callus guided by a quiescent center-related gene network

Ning Zhai[1,2,*], Xuan Pan[1,2,*], Minhuan Zeng[1] and Lin Xu[1,‡]

ABSTRACT

In plant tissue culture, callus formation is induced by a high auxin concentration. Among the three cell layers (the outer, middle and inner cell layers) of the callus, pluripotency acquisition in the middle cell layer is required for the potential ability of the callus to regenerate organs. Here, we reveal the developmental trajectory of middle cell layer initiation and maintenance in callus tissue originating from *Arabidopsis thaliana* hypocotyls. The S phase of the cell cycle is essential for the expression of quiescent center-related *SCARECROW* (*SCR*), *PLETHORA1* (*PLT1*) and *WUSCHEL-RELATED HOMEOBOX5* (*WOX5*) genes during the division of callus founder cells to initiate the callus primordium. After callus initiation, SHOOT-ROOT (SHR) proteins move from the inner to the middle cell layer and act together with SCR to promote the expression of *PLT1* and *WOX5*. *WOX5* represses the expression of *VASCULAR-RELATED NAC-DOMAIN* (*VND*) genes, thereby preventing callus tissue from differentiating into xylem cells. *PLT1* and *PLT2* directly activate *JACKDAW* (*JKD*), which is necessary for pluripotency acquisition in the middle cell layer. We hypothesize that the middle cell layer could have pluripotent stem cell activity and its establishment requires the quiescent center-related *SCR-SHR-WOX5-PLT1/2-JKD* gene network.

KEY WORDS: Plant regeneration, *De novo* organ regeneration, Callus, Tissue culture, Pluripotent stem cells, *Arabidopsis thaliana*

INTRODUCTION

Tissue culture, a widely used plant biotechnology for vegetative propagation, is based on the regenerative abilities of plants (Skoog and Miller, 1957; Ikeuchi et al., 2019). In the two-step tissue culture method of *Arabidopsis thaliana*, callus tissue forms from the vasculature of detached explants on callus-inducing medium (CIM) in response to a high concentration of auxin. Callus contains pluripotent cells that are competent for *de novo* organ regeneration, i.e. they can regenerate either roots on root-inducing medium (RIM) in response to a low auxin concentration, or shoots on shoot-inducing medium (SIM) in response to a high cytokinin concentration.

In *Arabidopsis*, the developmental pathway for vasculature-derived callus formation borrows from the pathways of lateral or adventitious root organogenesis in plants (Sugimoto et al., 2010, 2011; Duclercq et al., 2011; Fan et al., 2012; He et al., 2012; Liu et al., 2014). Therefore, the cellular structure of callus on CIM resembles that of the root primordium (RP) or the root apical meristem (RAM) (Sugimoto et al., 2010; Motte et al., 2014; Hu et al., 2017; Zhai and Xu, 2021). However, different from root organogenesis, in which the division of cells to form a mature root tip is strictly and developmentally controlled, callus exhibits more extensive cell division and it can be kept at the RP/RAM stage for a relatively long time by a high concentration of exogeneous auxin in the CIM.

Marker gene expression during callus formation in *Arabidopsis* has been extensively studied. Briefly, the regeneration-competent cells, which are vascular adult stem cells such as pericycle, procambium, and some vascular parenchyma cells (Che et al., 2007; Atta et al., 2009; Sugimoto et al., 2010, 2011; Liu et al., 2014; Hu et al., 2017) within detached explants, undergo cell fate transition to become callus founder cells by expressing *WUSCHEL-RELATED HOMEOBOX11* (*WOX11*) in response to a high concentration of auxin in the CIM (Liu et al., 2014; Hu et al., 2017). Then, callus founder cells divide to form the callus and express the RP/RAM identity genes *LATERAL ORGAN BOUNDARIES DOMAIN16* (*LBD16*), *PLETHORA1* and *2* (*PLT1*/*2*), *WOX5*/*7* and *SCARECROW* (*SCR*) (Di Laurenzio et al., 1996; Aida et al., 2004; Okushima et al., 2007; Gordon et al., 2007; Atta et al., 2009; Sugimoto et al., 2010; Fan et al., 2012; Liu et al., 2014; Kareem et al., 2015; Hu et al., 2017; Liu et al., 2018; Kim et al., 2018; Zhai and Xu, 2021). In this process, WOX11 is able to directly activate *LBD16* and *WOX5*/*7* expression (Hu and Xu, 2016; Sheng et al., 2017). *PLT3*/*5*/*7* are highly expressed in the callus during all stages of callus formation (Kareem et al., 2015). In addition, many epigenetic factors affect regeneration by regulating the expression of key genes in callus formation (Lee et al., 2018, 2019a, 2021; Kim et al., 2018; Ishihara et al., 2019; Wu et al., 2022).

Recently, we analyzed the single-cell transcriptome atlas in callus on CIM and found that the middle cell layer, which has quiescent center (QC)-like identity, plays a central role in pluripotency acquisition and, subsequently, in organ regeneration (Zhai and Xu, 2021). *PLT1*/*2* and *WOX5*/*7* are highly enriched in the middle cell layer of callus on CIM and promote auxin accumulation and cytokinin hypersensitivity, which are important for root or shoot organogenesis on RIM or SIM, respectively. In this study, we analyzed the developmental landscape of cell layer formation in callus tissue and revealed the gene network related to the QC in regulation of pluripotency acquisition in the middle cell layer.

RESULTS

Developmental trajectory of cell layer establishment in callus tissue

Using the ClearSee assay (Kurihara et al., 2015), we analyzed cell behavior and marker gene expression during callus formation from

[1]National Key Laboratory of Plant Molecular Genetics, CAS Center for Excellence in Molecular Plant Sciences, Institute of Plant Physiology and Ecology, Chinese Academy of Sciences, 300 Fenglin Road, Shanghai 200032, China. [2]University of Chinese Academy of Sciences, 19A Yuquan Road, Beijing 100049, China.
*These authors contributed equally to this work

‡Author for correspondence (xulin@cemps.ac.cn)

N.Z., 0000-0003-3688-2060; X.P., 0000-0001-6502-1783; L.X., 0000-0003-4718-1286

Handling Editor: Ykä Helariutta
Received 22 April 2022; Accepted 30 January 2023

Development (2023) 150, dev200879. doi:10.1242/dev.200879

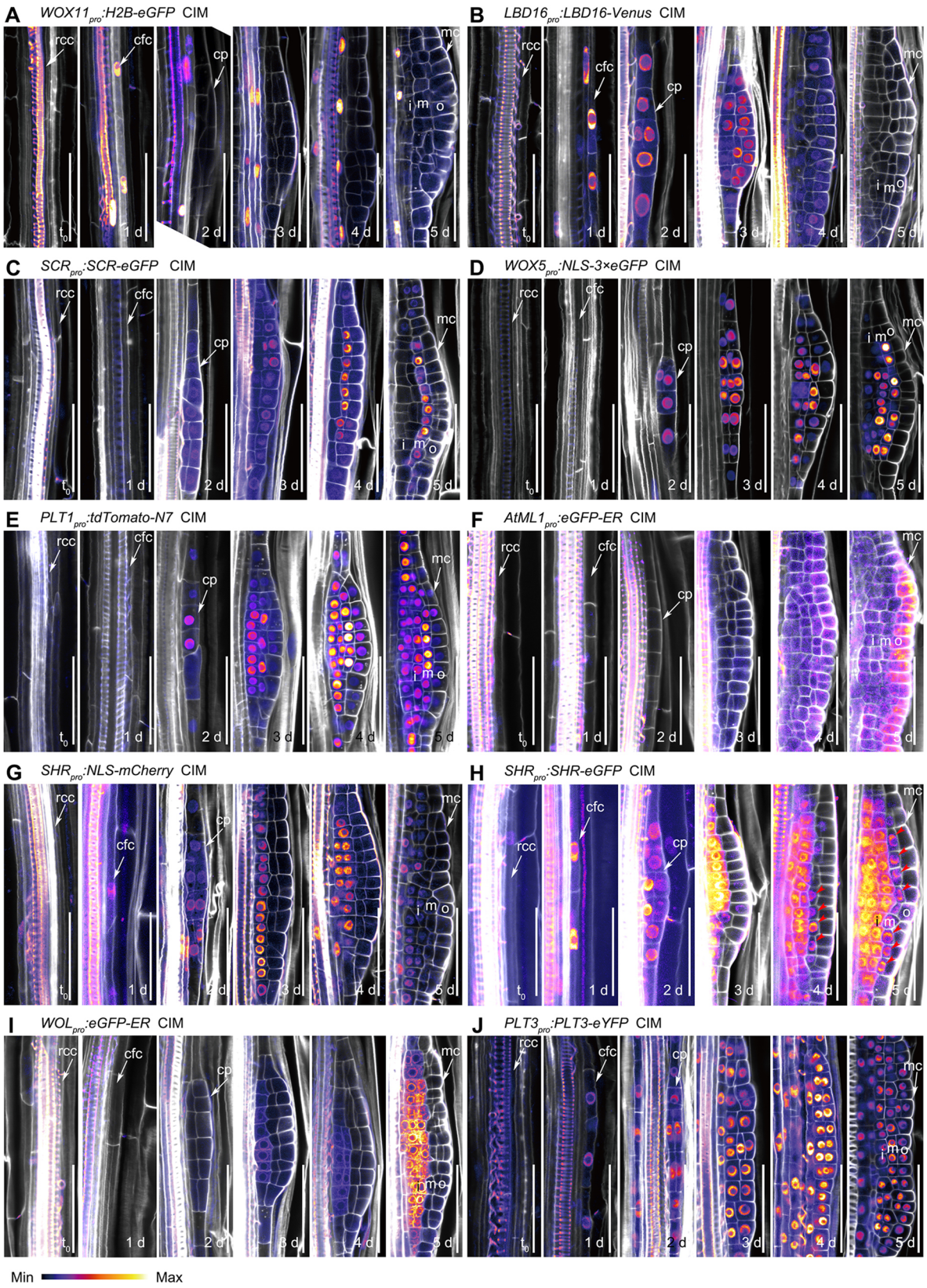

Fig. 1. Expression patterns of marker genes during callus formation on CIM. (A-J) Expression patterns of *WOX11*$_{pro}$*:H2B-eGFP* (A), *LBD16*$_{pro}$*:LBD16-Venus* (B), *SCR*$_{pro}$*:SCR-eGFP* (C), *WOX5*$_{pro}$*:NLS-3×eGFP* (D), *PLT1*$_{pro}$*:tdTomato-N7* (E), *ATML1*$_{pro}$*:eGFP-ER* (F), *SHR*$_{pro}$*:NLS-mCherry* (G), *SHR*$_{pro}$*:SHR-eGFP* (H), *WOL*$_{pro}$*:eGFP-ER* (I) and *PLT3*$_{pro}$*:PLT3-eYFP* (J) in callus forming from hypocotyl explants on CIM from time 0 (t_0) to 5 days. Red arrowheads in H indicate the nuclear-localized SHR-eGFP proteins, which are moved from the inner cell layer of the callus to the middle cell layer. cfc, callus founder cells; cp, callus primordium; d, days; i, inner cell layer of the callus; m, middle cell layer of the callus; mc, mature callus; o, outer cell layer of the callus; rcc, regeneration-competent cells. Scale bars: 50 µm.

Development (2023) 150, dev200879. doi:10.1242/dev.200879

hypocotyl explants of *Arabidopsis* (Fig. 1). Here, callus formation is described in four steps, borrowing the concept from root organogenesis (Xu, 2018): (1) the priming step, which involves the fate transition from regeneration-competent cells (i.e. the vascular adult stem cells) to callus founder cells at 1 day on CIM and does not require cell division; (2) the initiation step, which involves the division of callus founder cells to initiate the callus primordium at 2 days on CIM; (3) the patterning step, which involves continuous cell division in the callus primordium to form mature callus with three cell layers (i.e. inner, middle and outer cell layers) at 5 days; and (4) the maintenance of mature callus tissue, with further cell division and callus continuing to grow on CIM.

WOX11 transcripts were present in callus founder cells at 1 day and not in the callus primordium or mature callus from 2 days on CIM (Fig. 1A) (Liu et al., 2014; Hu et al., 2017). *LBD16* was expressed in callus founder cells at 1 day and callus primordium at 2 days, and then its expression level gradually decreased as the callus matured and formed three cell layers (Fig. 1B). Transcripts of *SCR*, *WOX5*/*7* and *PLT1*/*2* were not detected in callus founder cells at 1 day, but were detected in the callus primordium at 2 days (Fig. 1C-E; Fig. S1). High transcript levels of these genes were gradually restricted to the middle cell layer in mature callus at 5 days (Fig. 1C-E; Fig. S1). Lower transcript levels of *WOX5*/*7* and *PLT1*/*2* could be detected in some inner cell layers, but *SCR* transcripts were detected only in the middle cell layer (Fig. 1C-E; Fig. S1). The lower expression level of *PLT1*/*2* could also be observed in the outer cell layer in mature callus at 5 days (Fig. 1E; Fig. S1B). *ARABIDOPSIS THALIANA MERISTEM L1 LAYER* (*ATML1*) transcripts were not detected in the callus primordium, and were restricted to the outer cell layer during the formation of mature callus after 4 days (Fig. 1F). The promoter of the GRAS family gene *SHORT-ROOT* (*SHR*) (Helariutta et al., 2000) became active at the formation of callus founder cells at 1 day and callus primordium at 2 days, and then its activity was gradually restricted to the inner cell layer of mature callus at 5 days (Fig. 1G). Interestingly, the nuclear-localized SHR proteins were detected in callus founder cells at 1 day and callus primordium at 2 days as well as in the inner and middle cell layers of mature callus at 5 days (Fig. 1H), indicating that SHR proteins can move from the inner cell layer to the middle cell layer in mature callus (Nakajima et al., 2001). *WOODEN LEG* (*WOL*) (Mähönen et al., 2000) transcripts were not detected in the callus primordium, but were detected in the inner cell layer from 3 days during the formation of mature callus (Fig. 1I). *PLT3* transcripts were detected in many cells from callus founder cells to the three cell layers of mature callus (Fig. 1J). These data indicate that the middle cell layer markers in mature callus (i.e. *SCR*, *WOX5*/*7* and *PLT1*/*2* genes as well as SHR proteins) are also present in the callus primordium, whereas the outer and inner cell layer markers (*ATML1* and *WOL* genes) are not in the callus primordium and begin their expression during patterning of the callus.

We previously reported that the middle cell layer in mature callus exhibits a QC-like identity and is pluripotent for organ regeneration (Zhai and Xu, 2021). Analysis of previously published single-cell RNA sequencing (scRNA-seq) data (Zhai and Xu, 2021) confirmed that cells co-expressing the QC-related gene network *SCR*, *WOX5* and *PLT1*/*2* were present in the middle cell layer (cell cluster 2 in Fig. 2A). We further tested three QC markers (QC25, QC184 and QC46) (Sabatini et al., 2003) during callus formation. The result showed that the β-glucuronidase (GUS) signals of QC25 and QC184 were highly concentrated in the middle cell layer (Fig. 2B,C) (for QC25 analysis in callus, see also Atta et al., 2009). We did not

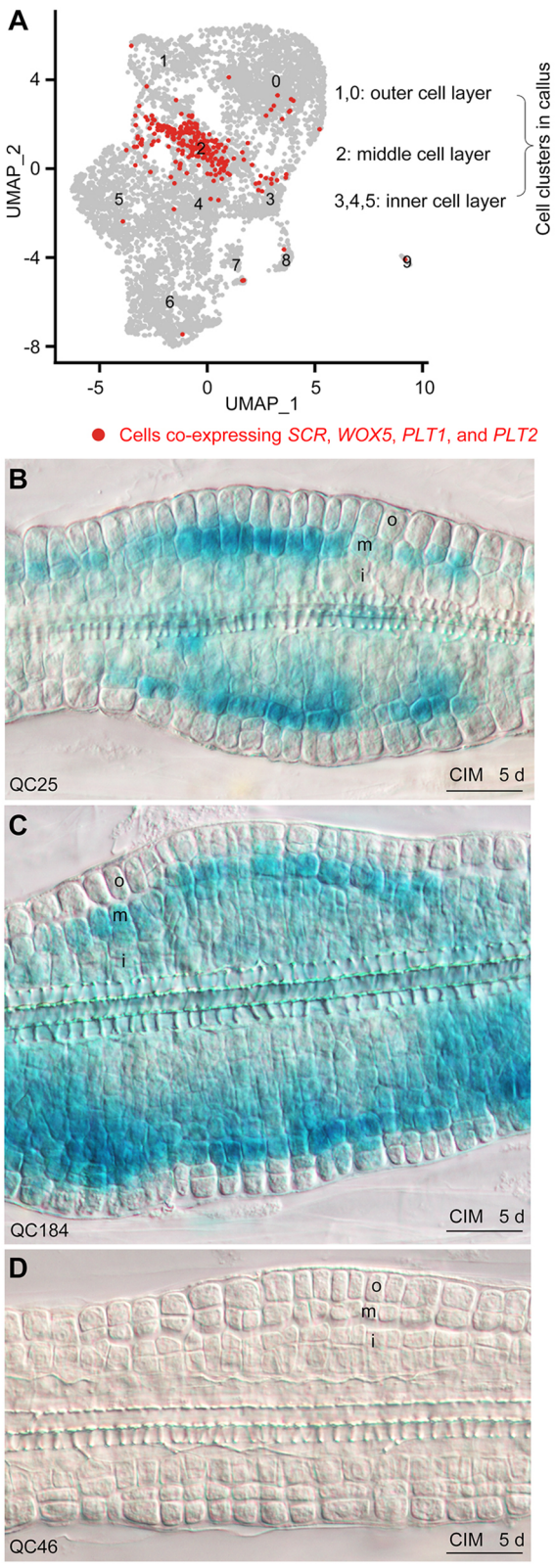

Fig. 2. QC-like identity establishment in the middle cell layer of the callus. (A) scRNA-seq analysis of cells co-expressing *SCR*, *WOX5* and *PLT1*/*2* marker genes in the middle cell layer of mature callus. scRNA-seq data were obtained from our previous study (Zhai and Xu, 2021). (B-D) Expression patterns of QC25 (B), QC184 (C) and QC46 (D) in callus cultured on CIM for 5 days. d, days; i, inner cell layer of the callus; m, middle cell layer of the callus; o, outer cell layer of the callus. Scale bars: 20 µm.

Development (2023) 150, dev200879. doi:10.1242/dev.200879

find a QC46 signal in mature callus (Fig. 2D), and all three GUS markers were absent in the callus primordium. Therefore, the QC-like identity is progressively obtained in the middle cell layer during callus patterning.

Completion of S phase in callus founder cells ensures callus initiation

To study the cell cycle process during the initiation of the callus primordium from callus founder cells, we treated hypocotyl explants with the S-phase inhibitor hydroxyurea (HU) (Cools et al., 2010) and the M-phase inhibitor nocodazole (NOCO) (Fig. S2). Treatment with either HU or NOCO blocked cell division in callus founder cells (Fig. 3A,B).

WOX11 and *LBD16* were expressed normally under HU or NOCO treatment, indicating that the establishment of callus founder cells in the priming step might not be dependent on entry into the cell cycle (Fig. 3A,B). Expression of *SCR*, *WOX5* and *PLT1* was blocked by HU treatment, but not by NOCO treatment (Fig. 3A,B). These results indicate that S phase, but not M phase, is essential for the activation of *SCR*, *WOX5* and *PLT1* expression and for the fate transition from callus founder cells to callus primordium.

Interestingly, when callus founder cells were arrested at the M phase by NOCO treatment, the nuclei continuously propagated and the cell continuously expanded. However, the cell could not divide, resulting in a huge syncytium-like structure with mixed expression of *WOX11* and *WOX5* (Fig. 3C). After the NOCO treatment was withdrawn from CIM, new cell plates could form between the nuclei in the syncytium-like structure (Fig. 3D-F). After the formation of new cell plates, decreased *WOX11* expression and continuous *WOX5* expression were observed in the syncytium-like structure (Fig. 3F). These findings indicate that auxin promotes repeated chromatin replication regardless of M-phase completion in callus founder cells, and that *WOX11* expression may cease after the completion of callus founder cell division.

SCR and SHR promote middle cell layer formation in callus

To analyze the role of the SCR-SHR complex in the middle cell layer of callus, we first observed the regeneration phenotypes of *shr-2* and *scr-6* mutants. Shooting ability was almost lost in the callus of *shr-2*

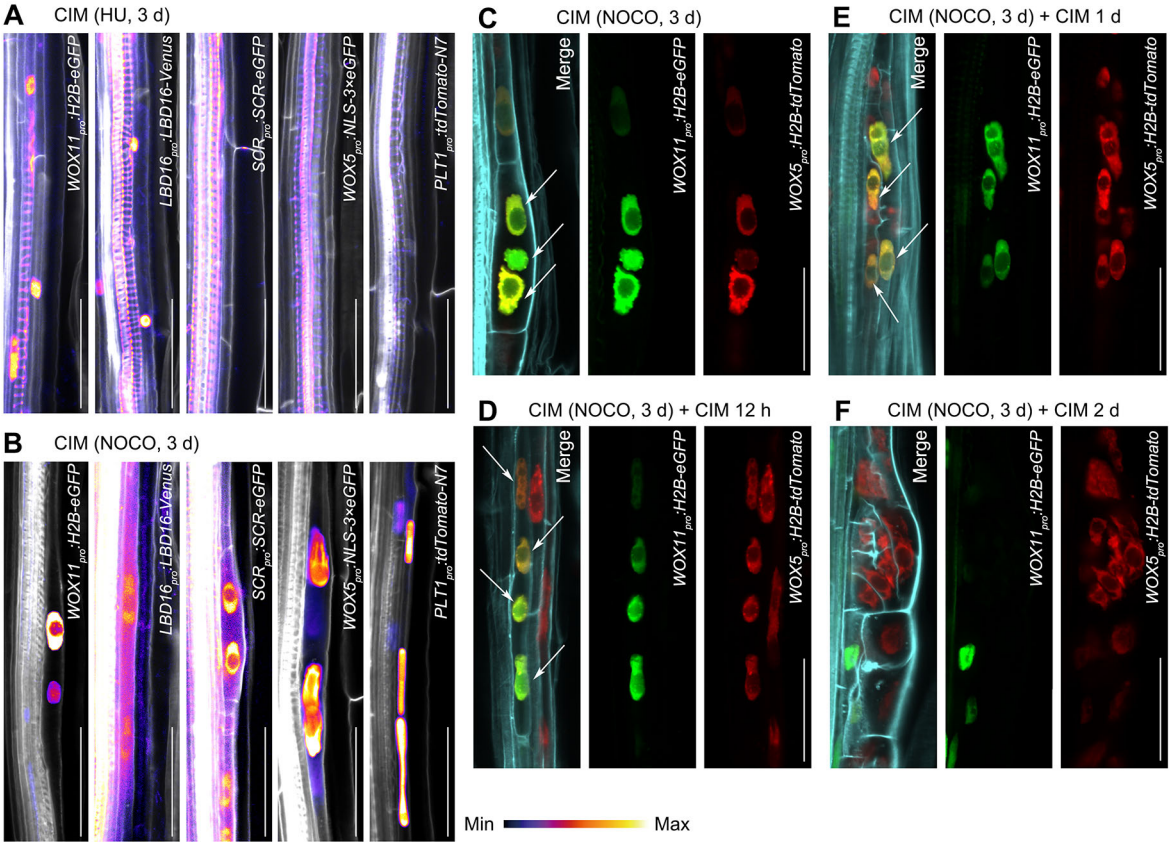

Fig. 3. Effects of S-phase inhibitor HU and M-phase inhibitor NOCO treatments on callus primordium initiation. (A,B) Expression patterns of *WOX11*$_{pro}$*:H2B-eGFP*, *LBD16*$_{pro}$*:LBD16-Venus*, *SCR*$_{pro}$*:SCR-eGFP*, *WOX5*$_{pro}$*:NLS-3×eGFP* and *PLT1*$_{pro}$*:tdTomato-N7* in callus derived from hypocotyl explants cultured on CIM for 3 days with 75 mM HU (A) or 40 µM NOCO (B). We examined more than ten samples for *WOX11*$_{pro}$*:H2B-eGFP* and *LBD16*$_{pro}$*:LBD16-Venus* under HU or NOCO treatment, and all of them showed positive fluorescent signals; more than ten samples for *SCR*$_{pro}$*:SCR-eGFP* and *PLT1*$_{pro}$*:tdTomato-N7* under HU or NOCO treatment, and all of them showed negative (HU treatment) or positive (NOCO treatment) fluorescent signals; and 12 samples for *WOX5*$_{pro}$*:NLS-3×eGFP* under HU or NOCO treatment, of which eight showed negative fluorescent signals under HU treatment and all showed positive fluorescent signals under NOCO treatment. See Fig. 1 for controls with no chemical treatment. (C) Co-expression of *WOX11*$_{pro}$*:H2B-eGFP* and *WOX5*$_{pro}$*:H2B-tdTomato* in callus derived from hypocotyl explants cultured on CIM for 3 days with 40 µM NOCO treatment. Arrows indicate co-expression of *WOX11* and *WOX5* in a syncytium-like cell with three nuclei. We examined ten samples, and all of them showed co-expression of *WOX11* and *WOX5*. (D-F) Expression of *WOX11*$_{pro}$*:H2B-eGFP* and *WOX5*$_{pro}$*:H2B-tdTomato* in callus derived from hypocotyl explants cultured on CIM for 3 days with 40 µM NOCO treatment and then on CIM without NOCO for another 12 h (D), 1 day (E) and 2 days (F). Arrows indicate co-expression of *WOX11* and *WOX5* in syncytium-like cells (D,E). New cell plates formed to separate nuclei in the syncytium-like cell at 1 d after removal of NOCO treatment (E), and downregulation of *WOX11* in the syncytium-like cell was observed at 2 days after removal of NOCO treatment (F). d, days; h, hours. Scale bars: 50 µm.

Development (2023) 150, dev200879. doi:10.1242/dev.200879

or *scr-6* when moved to SIM (Fig. 4A-D) (for analysis of *SCR* in shoot regeneration, see also Kim et al., 2018). Rooting ability was also lost in *scr-6* and significantly reduced in *shr-2* when callus was moved to RIM (Fig. 4E). Therefore, *SCR* and *SHR* may be crucially involved in pluripotency acquisition in the callus.

Both *shr-2* and *scr-6* calli lost the normal pattern of three cell layers (Fig. 4F-Q). However, calli of the *shr-2* and *scr-6* mutants showed different phenotypes on CIM. Callus cell division was faster in *shr-2* (Fig. 4J-M) but slower in *scr-6* (Fig. 4N-Q) compared with Col-0 callus (Fig. 4F-I). Abnormal cell plate formation could be observed in *scr-6* callus (Fig. 4N-Q).

Next, we analyzed the expression patterns of marker genes in the calli of *shr-2* and *scr-6*. Compared with their expression patterns in the wild-type background (Figs 1C-E, 2B), *WOX5*, *PLT1* and QC25 showed decreased expression levels and discontinuous expression patterns in the *shr-2* mature callus, and *SCR* expression was barely detected in the *shr-2* mature callus (Fig. 4R-U). *WOX5* showed a decreased expression level and a discontinuous expression pattern in the *scr-6* mature callus, and *PLT1* and QC25 were barely detected in the *scr-6* mature callus (Fig. 4V-X).

Together, these data indicate that the QC-like identity was partially lost in *shr-2* and *scr-6* mature calli on CIM, leading to loss

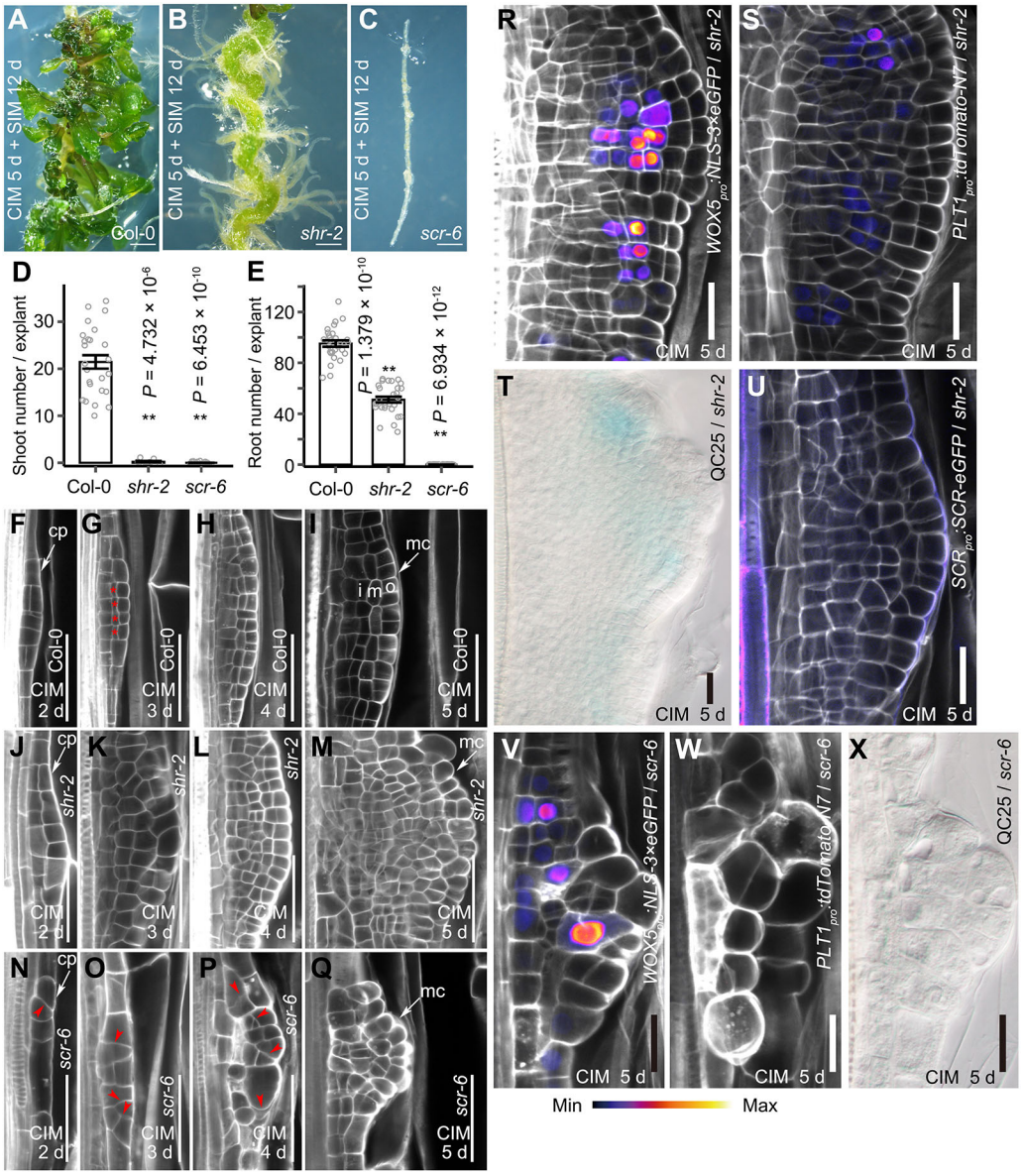

Fig. 4. Roles of *SCR* and *SHR* in establishment of the middle cell layer. (A-C) Shoot regeneration at 12 days on SIM from callus derived from Col-0 (A), *shr-2* (B) or *scr-6* (C). (D,E) Statistical analysis of shoot regeneration on SIM at 12 days (D) and root regeneration on RIM at 8 days (E) from callus derived from Col-0, *shr-2* or *scr-6*. Calli were cultured on CIM for 5 days and then moved to SIM (A-D) or RIM (E). Data are mean±s.e.m. (*n*=24 explants). Circles represent individual values. ***P*<0.01 (two-tailed Mann–Whitney *U*-test compared with Col-0 control). (F-Q) Analysis of cell division in 2- to 5-day callus on CIM from Col-0 (F-I), *shr-2* (J-M) and *scr-6* (N-Q). Red asterisks indicate the formation of the middle cell layer in Col-0 (G). Red arrowheads indicate abnormal cell plate formation during callus formation in *scr-6* (N-P). (R-U) Expression patterns of *WOX5*$_{pro}$*:NLS-3×eGFP* (R), *PLT1*$_{pro}$*:tdTomato-N7* (S), QC25 (T) and *SCR*$_{pro}$*:SCR-eGFP* (U) in 5-day callus on CIM derived from *shr-2*. For controls, see Figs 1C-E and 2B. (V-X) Expression patterns of *WOX5*$_{pro}$*:NLS-3×eGFP* (V), *PLT1*$_{pro}$*:tdTomato-N7* (W) and QC25 (X) in 5-day callus on CIM derived from *scr-6*. For controls, see Figs 1D,E and 2B. cp, callus primordium; d, days; i, inner cell layer of the callus; m, middle cell layer of the callus; mc, mature callus; o, outer cell layer of the callus. Scale bars: 1 mm (A-C); 50 µm (F-Q); 20 µm (R-X).

Development (2023) 150, dev200879. doi:10.1242/dev.200879

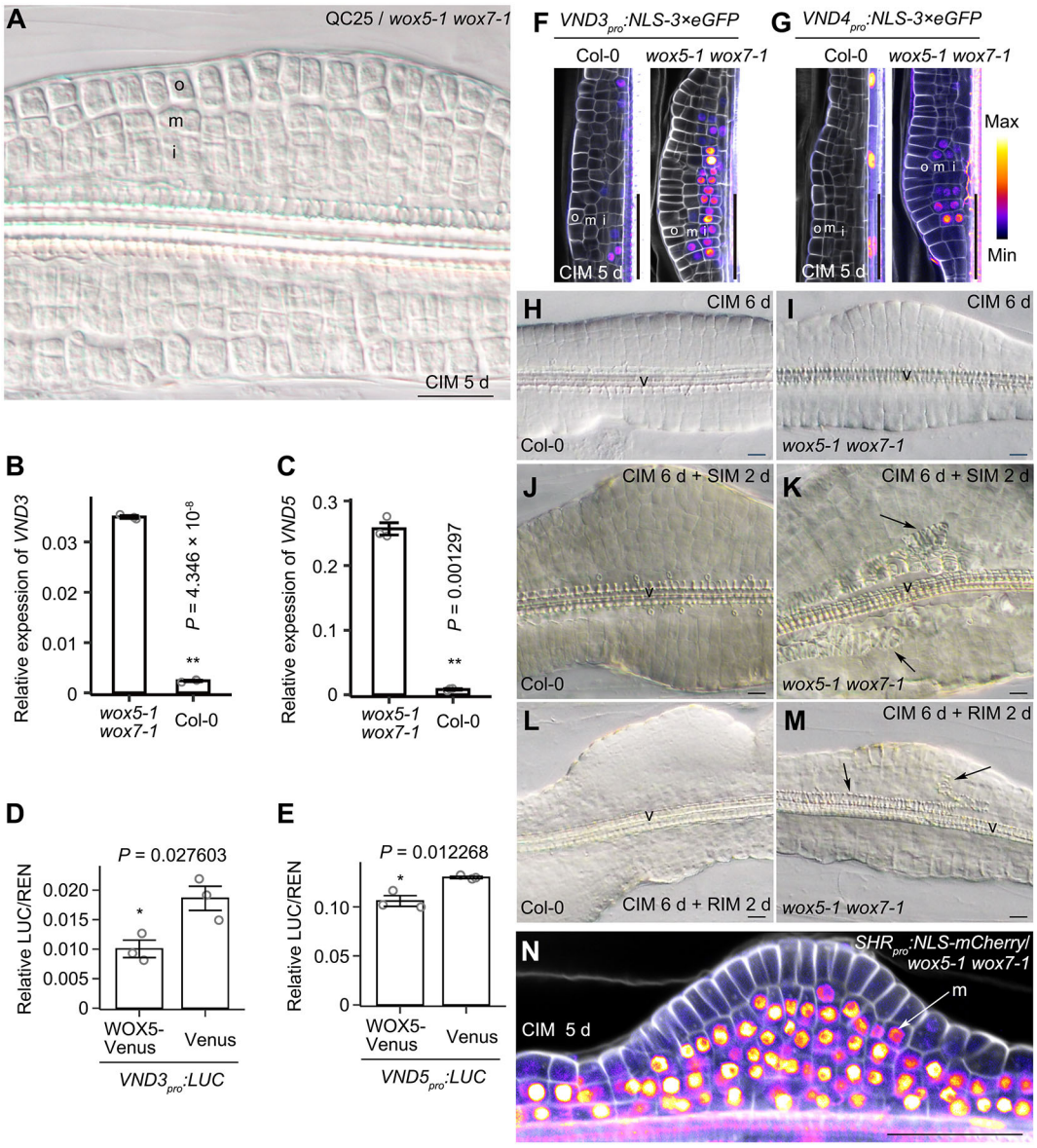

Fig. 5. Roles of *WOX5/7* in the middle cell layer of the callus. (A) Expression of QC25 in 5-day callus derived from *wox5-1 wox7-1* on CIM. See Fig. 2B for QC25 in the wild-type control. (B,C) qRT-PCR analysis of *VND3* (B) and *VND5* (C) transcript levels in 5-day callus on CIM derived from *wox5-1 wox7-1* compared with callus derived from Col-0. Data are mean±s.e.m. from three biological replicates. Each biological replicate was analyzed with three technical replicates. Individual values are indicated by circles. $^{**}P<0.01$ (two-tailed Student's *t*-test). (D,E) Relative ratio of firefly luciferase (LUC) to *Renilla* luciferase (REN) activity in *Arabidopsis* protoplasts co-transformed with $VND3_{pro}$*:LUC* (D) or $VND5_{pro}$*:LUC* (E) with $UBQ10_{pro}$*:WOX5-Venus* or $UBQ10_{pro}$*:Venus*. Data are mean±s.e.m. from three biological replicates. Each biological replicate was analyzed with two technical replicates. Individual values are indicated by circles. $^{*}P<0.05$ (two-tailed Student's *t*-test). (F,G) Expression patterns of $VND3_{pro}$*:NLS-3×eGFP* (F) and $VND4_{pro}$*:NLS-3×eGFP* (G) in 5-day callus on CIM derived from Col-0 or *wox5-1 wox7-1*. (H-M) Analysis of xylem differentiation in callus on CIM (H,I), SIM (J,K) or RIM (L,M) from hypocotyl explants of Col-0 (H,J,L) or *wox5-1 wox7-1* (I,K,M). Calli were cultured on CIM for 6 days (H,I) and then moved to SIM for 2 days (J,K) or RIM for 2 days (L,M). Arrows indicate ectopic xylem formation. (N) Expression pattern of SHR_{pro}*:NLS-mCherry* in *wox5-1 wox7-1*. Hypocotyl explants were cultured on CIM for 5 days. For control, see Fig. 1G. d, day; i, inner cell layer of the callus; m, middle cell layer of the callus; o, outer cell layer of the callus. v, vasculature of explants. Scale bars: 20 µm (A); 50 µm (F,G,N); 10 µm (H-M).

of pluripotency for organ regeneration. In addition, SCR and SHR might have additional roles independent of the SCR-SHR complex in the callus middle cell layer.

WOX5/7 maintain the identity of the middle cell layer by preventing vascular differentiation

Our recent study showed that *WOX5/7* are involved in pluripotency acquisition in callus via the promotion of auxin accumulation and cytokinin hypersensitivity on CIM (Zhai and Xu, 2021). We found that the QC marker QC25 lost its expression in the *wox5-1 wox7-1* callus (Fig. 5A). In addition, RNA-seq data of calli from *wox5-1 wox7-1* and Col-0 (Zhai and Xu, 2021) and *SCR* marker line analysis showed that the *SCR* expression level was reduced in the middle cell layer of *wox5-1 wox7-1* callus compared with Col-0 callus (Fig. S3A,B). Therefore, QC-like identity is partially lost in the middle cell layer of *wox5-1 wox7-1* callus.

The transcript levels of the *VASCULAR-RELATED NAC-DOMAIN* (*VND*) genes *VND3* and *VND5* were higher in *wox5-1*

Development (2023) 150, dev200879. doi:10.1242/dev.200879

wox7-1 callus than in wild-type callus (Fig. 5B,C) (Zhai and Xu, 2021). In addition, WOX5 was able to repress the expression of *VND3* and *VND5* in the *in vitro* protoplast assay (Fig. 5D,E). The *VND3* and *VND4* marker lines (*VND3*$_{pro}$*:NLS-3×eGFP* and *VND4*$_{pro}$*:NLS-3×eGFP*) showed that *VND3*/*4* were ectopically expressed in the middle and inner cell layers of *wox5-1 wox7-1* callus compared with wild-type callus (Fig. 5F,G). *VND* genes are involved in the differentiation of xylem vessel elements (Kubo et al., 2005). We observed that ectopic xylem formation occurred in the callus of *wox5-1 wox7-1* when it was moved to SIM or RIM, but not when it was on CIM (Fig. 5H-M). We hypothesize that a high level of auxin in CIM might prevent xylem differentiation although VND genes were ectopically expressed in *wox5-1 wox7-1* callus (Lee et al., 2019b). Induced overexpression of *VND3* or *VND4* fused with the repression domain SRDX (Hiratsu et al., 2003) (*pER8:gVND3-SRDX* or *pER8:gVND4-SRDX*) on CIM could repress the ectopic xylem formation in the *wox5-1 wox7-1* callus (Fig. S3C).

We also observed that the *SHR* promoter, which was active in the inner cell layer of wild-type callus (Fig. 1G), was ectopically activated in the middle cell layer of the *wox5-1 wox7-1* callus on CIM (Fig. 5N). The inner cell layer of the callus has vascular initial identity (Zhai and Xu, 2021), and the *SHR* promoter is active in the vasculature of root tips (Helariutta et al., 2000; Nakajima et al., 2001).

Together, these data suggest that *WOX5*/*7* may maintain the identity of the middle cell layer and prevent cell differentiation into vasculature.

PLT1/*2* activate *JKD* in the middle cell layer

We previously showed that PLT1/2 could form a protein complex with WOX5/7 to promote auxin biosynthesis in the middle cell layer of callus on CIM (Zhai and Xu, 2021). Further analyses of the RNA-seq data from Col-0 and *plt1-21 plt2-21* calli on CIM revealed that *JKD*, which encodes a zinc finger protein, was downregulated in *plt1-21 plt2-21* callus compared with Col-0 callus (Zhai and Xu, 2021) (Fig. 6A,B). Gene ontology (GO) analysis indicates that the expression levels of genes involved in asymmetric cell division, root cap development, regulation of meristem growth, auxin biosynthetic process, and gibberellin biosynthetic process were downregulated in *plt1-21 plt2-21* callus, and *JKD* was annotated to be involved in asymmetric cell division and regulation of meristem growth (Welch et al., 2007) (Fig. 6B). qRT-PCR confirmed that *JKD* was downregulated in *plt1-21 plt2-21* callus compared with Col-0 callus (Fig. 6C). PLT2-YFP was able to directly bind to the *JKD* locus (Fig. 6D) in ChIP-seq analysis (Santuari et al., 2016). We also showed that PLT1 was able to activate *JKD* expression in the *in vitro* protoplast assay (Fig. 6E).

Analysis of the *JKD* marker line (*JKD*$_{pro}$*:JKD-eYFP*) showed that *JKD* expression started in the callus primordium at 2 days of culture, and a high expression level was detected in the middle cell layer of mature callus at 5 days on CIM (Fig. 6F). A lower expression level of *JKD* could also be detected in the outer cell layer of mature callus at 5 days (Fig. 6F). The *JKD*$_{pro}$*:JKD-eYFP* marker line indicated that *JKD* was also present in the middle cell layer of *plt1-21 plt2-21* mature callus on CIM (Fig. 6G), but its expression level was lower in the middle cell layer of *plt1-21 plt2-21* callus compared with Col-0 callus (Fig. 6G,H).

A mutation in *JKD* resulted in significantly reduced shoot or root regeneration from callus on SIM or RIM, respectively (Fig. 6I,J) (for analysis of *JKD* in shoot regeneration, see also Wu et al., 2022). In addition, *JKD* overexpression could partially rescue the root and shoot regeneration defects of *plt1-21 plt2-21* callus (Fig. S4).

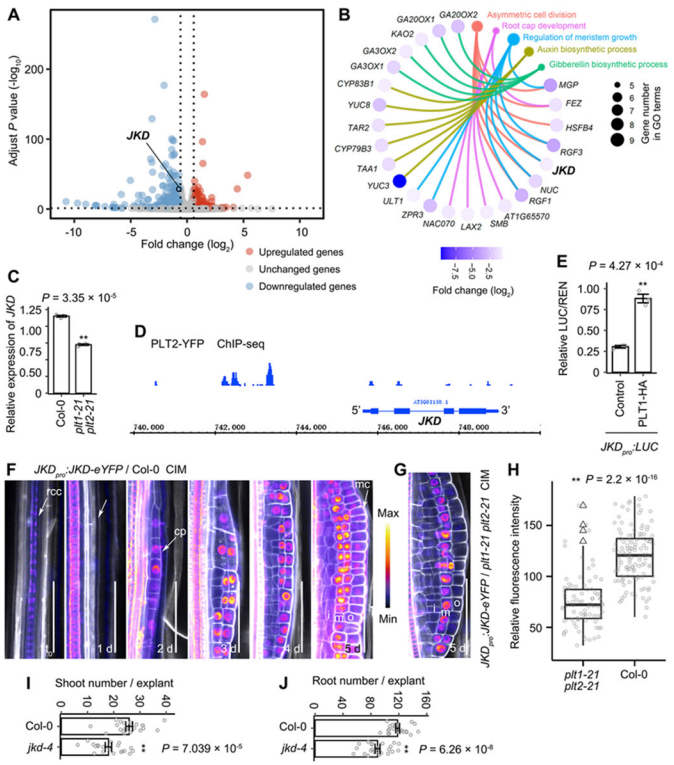

Fig. 6. Roles of PLT1/2 in promotion of *JKD*. (A) RNA-seq analysis of gene transcript profiles in callus derived from Col-0 or *plt1-21 plt2-21* hypocotyl explants on CIM at 6 days. *JKD* was among the genes with lower transcript levels in *plt1-21 plt2-21* than in Col-0. The RNA-seq data for *plt1-21 plt2-21* have been reported previously (Zhai and Xu, 2021). (B) Selected GO analysis of downregulated genes in *plt1-21 plt2-21* callus compared with Col-0 callus. (C) qRT-PCR analysis of *JKD* in 5-day callus on CIM derived from *plt1-21 plt2-21* compared with callus derived from Col-0. Data are mean ±s.e.m. from three biological replicates. Each biological replicate was analyzed with three technical replicates. Individual values are indicated by circles. ***P*<0.01 (two-tailed Student's *t*-test). (D) ChIP-seq analysis of PLT2-YFP on the *JKD* locus. The ChIP-seq data were previously reported (Santuari et al., 2016). (E) Relative ratio of firefly luciferase (LUC) to *Renilla* luciferase (REN) activity in *Arabidopsis* protoplasts co-transformed with *JKD*$_{pro}$*:LUC* without (control) or with *35S*$_{pro}$*:PLT1-HA*. Data are mean±s.e.m. from three biological replicates. Each biological replicate was analyzed with two technical replicates. Individual values are indicated by circles. ***P*<0.01 (two-tailed Student's *t*-test). (F,G) Expression pattern of *JKD*$_{pro}$*:JKD-YFP* in Col-0 callus cultured on CIM from t_0 to 5 days (F) or in *plt1-21 plt2-21* callus cultured on CIM for 5 days (G). (H) Relative fluorescence intensity of *JKD*$_{pro}$*:JKD-YFP* in the middle cell layers of 5-day Col-0 callus and *plt1-21 plt2-21* callus cultured on CIM. The fluorescence intensity was calculated using nuclei from the middle layer cell (*n*=87 for *plt1-21 plt2-21* and *n*=124 for Col-0) using Nikon C2 NIS-Element software. ***P*<0.01 by two-tailed Student's *t*-test. The box bounds indicate the interquartile range (25th to 75th percentiles), the center line indicates the median, the whiskers indicate 1.5× the interquartile range from the lower and upper bounds, and the outliers are indicated by triangles. The individual values are indicated by circles. (I,J) Statistical analysis of shoot regeneration on SIM at 12 days (I) and root regeneration on RIM at 8 days (J) from callus derived from Col-0 and *jkd-4*. Hypocotyl explants were cultured on CIM for 6 days and then moved to SIM or RIM. Data are mean±s.e.m. (*n*=24 explants). Individual values are indicated by circles. ***P*<0.01 (two-tailed Mann–Whitney *U*-test). d, days; cp, callus primordium; i, inner cell layer of the callus; m, middle cell layer of the callus; mc, mature callus; o, outer cell layer of the callus; rcc, regeneration-competent cells. Scale bars: 50 µm.

Together, these data indicate that PLT1/2 might directly activate *JKD* in the middle cell layer for organ regeneration.

Development (2023) 150, dev200879. doi:10.1242/dev.200879

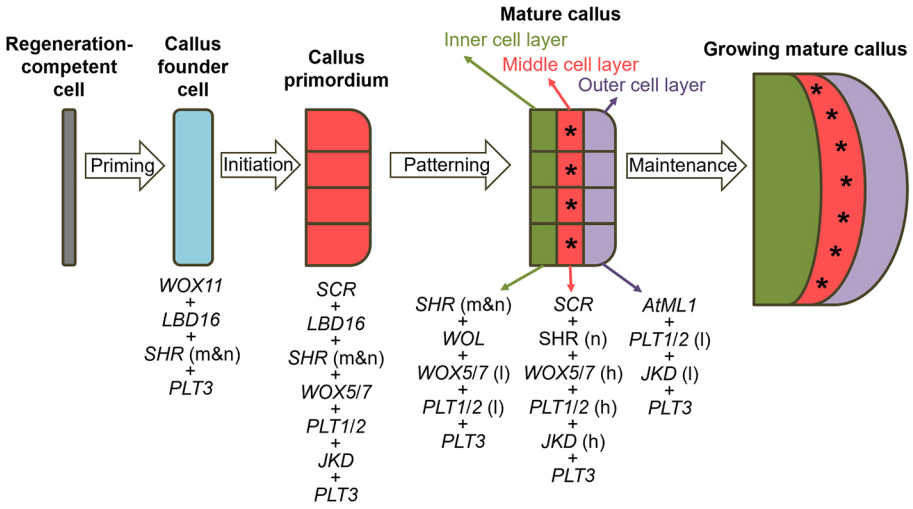

Fig. 7. Gene expression patterns during callus formation. Schematic of the four steps of callus formation on CIM, with marker genes or proteins for each step. h, higher expression level; l, lower expression level; m, mRNA; n, nuclear protein. Note that *PLT3* is expressed in almost all cells from callus founder cell to mature callus. PSCs are formed in the middle cell layer of mature callus, indicated by asterisks.

DISCUSSION

Pluripotent stem cells in the middle cell layer of callus

Studies from animals show that pluripotent stem cells (PSCs) are able to self-renew and differentiate into all cell types found in the adult organism, whereas multipotent or unipotent stem cells can only differentiate into specific cell type(s) in tissues (Robinton and Daley, 2012; De Los Angeles et al., 2015; Sang et al., 2018). We propose that PSCs exist in the middle cell layer of mature callus in tissue culture on the basis of the following evidence: (1) those cells are able to self-renew, as indicated by their maintenance in a pluripotent state on CIM; and (2) those cells can form the stem cell niche of either the RAM on RIM or the shoot apical meristem on SIM, thereby producing almost all cell types found in the adult plant. However, plant PSCs in callus tissue do not exhibit embryonic features, and this differs from PSCs in animals (Robinton and Daley, 2012; De Los Angeles et al., 2015).

PSCs in the middle cell layer of callus have a QC-like identity to some extent, because the transcriptome and marker gene expression in the middle cell layer resemble that of the QC in the root apical meristem (Zhai and Xu, 2021). In addition, the gene network that is essential for QC identity is also required for PSC establishment in the middle cell layer. However, PSCs are not equivalent to the QC. There are many differences in the transcriptome between the two types of cells, and cell division is highly activated in PSCs of callus but not in the QC (Zhai and Xu, 2021).

Developmental framework of callus formation

In this study, we examine in detail the cell lineage during establishment of three cell layers in callus on CIM (summarized in Fig. 7). In the priming step, the regeneration-competent cell undergoes cell fate transition to form the callus founder cell at around 1 day on CIM by expressing *WOX11* and *LBD16*. In the initiation step, the long, bar-shaped callus founder cell mainly undergoes anticlinal cell divisions to form the callus primordium with small, square-shaped cells. In this step, *SCR*, *SHR* (both mRNA and nuclear protein), *WOX5/7*, *PLT1/2* and *JKD* are expressed in the callus primordium, and the upregulation of *SCR*, *WOX5* and *PLT1* is dependent on the callus founder cell entering S phase. *WOX11* expression decreases dependent on the completion of callus founder cell division. *LBD16* is also highly expressed in the callus primordium independently of S phase. In the patterning step, the cells of the callus primordium further undergo rapid cell division with pattern establishment of marker genes to form mature callus with three cell layers. Periclinal cell divisions lead to the separation of the inner cell layer expressing the marker genes *SHR* (mRNA) and *WOL*. Some cells in the inner cell layer also show relatively lower expression of *WOX5/7* and *PLT1/2*. Then, periclinal cell divisions further lead to separation of the outer cell layer expressing the marker gene *ATML1*. Some cells in the outer cell layer also show relatively lower expression of *JKD* and *PLT1/2*. The middle cell layer acquires QC-like identity by high expression levels of *SCR*, *WOX5/7*, *PLT1/2* and *JKD*, as well as the SHR proteins.

By molecular analysis, we show that QC-related genes form a regulatory network to promote middle cell layer establishment on CIM. *SCR* and *WOX5* might form a positive-activation loop in the middle cell layer (Shimotohno et al., 2018). SHR-SCR promotes the expression of *PLT1*. WOX5/7 prevent cell differentiation by repressing the expression of *VND* genes, which are involved in xylem differentiation. PLT1/2 directly promote *JKD* expression. Further identification of key genes and exploration of the gene regulatory network in regulation of PSCs in the middle cell layer of callus will be important to understand pluripotency acquisition and organ regeneration in tissue culture.

MATERIALS AND METHODS

Plant materials and culture conditions

Arabidopsis Col-0 was used as wild type in this study. *$WOX11_{pro}$:H2B-eGFP* (Zhai and Xu, 2021), *$WOX5_{pro}$:NLS-3×eGFP* (Zhai and Xu, 2021), *$PLT1_{pro}$:tdTomato-N7* (Zhai and Xu, 2021), *$ATML1_{pro}$:eGFP-ER* (Gordon et al., 2007), *SHR_{pro}:NLS-mCherry* (Marquès-Bueno et al., 2016), *SHR_{pro}:SHR-eGFP* (Wu et al., 2014), *WOL_{pro}:eGFP-ER* (Gordon et al., 2009), *$PLT3_{pro}$:PLT3-eYFP* (Kareem et al., 2015), *JKD_{pro}:JKD-eYFP* (Wu et al., 2022), *SCR_{pro}:SCR-eGFP/scr-4* (Ws background) (Gallagher et al., 2004), QC25, QC46, QC184 (Sabatini et al., 2003), *wox5-1 wox7-1* (Hu and Xu, 2016), *plt1-21 plt2-21* (Zhai and Xu, 2021), *jkd-4* (Welch et al., 2007) and *shr-2* (Nakajima et al., 2001) have been described previously. For construction of *$LBD16_{pro}$:LBD16-Venus*, the 4.8-kb promoter and the gene body of *LBD16* fused with Venus were cloned into pBI101 to replace the *GUS* gene. For construction of *$WOX7_{pro}$:NLS-3×eGFP*, *$VDN3_{pro}$:NLS-3×eGFP*, *$VDN4_{pro}$:NLS-3×eGFP*, *$WOX5_{pro}$:H2B-tdTomato* and *$PLT2_{pro}$:tdTomato-N7*, the 3.5-kb promoter of *WOX7*, 2.9-kb promoter of *VDN3*, 3.3-kb promoter of *VDN4*, 4.5-kb promoter of *WOX5* and 5.8-kb promoter of *PLT2* were cloned into pBI101-NLS-3×eGFP, pBI101-H2B-tdTomato and pBI101-tdTomato-N7 (modified from pBI101, Clontech). For construction of *pER8:gVND3-SRDX*, *pER8:gVND4-SRDX* and *pER8:JKD*, the genomic

gene bodies encoding *VND3* and *VND4* fused with *SRDX* and the cDNA encoding *JKD* were each cloned into pER8 (Zuo et al., 2000).

Tissue culture was performed as previously described using hypocotyls as explants (Zhai and Xu, 2021). The cell cycle inhibitors were HU (H8627, Sigma-Aldrich) and NOCO (ab120630, Abcam). The role of NOCO treatment was confirmed by the Cytrap line (Yin et al., 2014) (Fig. S2).

qRT-PCR, *in vitro* protoplast assay, GUS staining and ClearSee assay

qRT-PCR and GUS staining were carried out as previously described (He et al., 2012). The qRT-PCR results are presented as relative transcript levels, normalized against that of *ACTIN*.

To construct firefly luciferase reporter vectors, the 2.9-kb promoter of *VND3*, the 3.2 kb-promoter of *VND5* and the 5-kb promoter of *JKD* were cloned into pAB287 containing the *LUC* coding sequence. For the *in vitro* protoplast assay, $UBQ10_{pro}$*:WOX5-Venus* and $35S_{pro}$*:PLT1-HA* have been described previously (Zhai and Xu, 2021).

The ClearSee assay was performed following previously reported protocols (Kurihara et al., 2015; Zhang et al., 2019; Zhai and Xu, 2021). The Nikon C2 software NIS-Element was used to export 8-bit gray images. ImageJ was used to convert grayscale images to color images by means of a lookup table. This allowed for the comparison of fluorescence levels within but not between images. For marker gene expression, two biological repeats were analyzed and showed similar results.

The primers used for molecular cloning and PCR are listed in Table S1.

Gene sequences

Gene sequences were accessed from the Arabidopsis Genome Initiative (https://www.arabidopsis.org/): *WOX11* (AT3G03660), *LBD16* (AT2G42430), *WOX5* (AT3G11260), *WOX7* (AT5G05770), *PLT1* (AT3G20840), *PLT2* (AT1G51190), *PLT3* (AT5G10510), *SCR* (AT3G54220), *SHR* (AT4G37650), *JKD* (AT5G03150), *ATML1* (AT4G21750) and *WOL* (AT2G01830).

Acknowledgements

We thank L. Sheng and Y. Ge for technical assistance in this research. We thank B. Scheres, S. Wu, J.-W. Wang, and ABRC for *Arabidopsis* seeds used in this work.

Competing interests

The authors declare no competing or financial interests.

Author contributions

Conceptualization: N.Z., L.X.; Validation: N.Z., X.P., M.Z.; Investigation: N.Z., X.P., M.Z.; Writing - original draft: L.X.; Funding acquisition: L.X.

Funding

This work was supported by grants from the National Natural Science Foundation of China (32225007), the Strategic Priority Research Program of the Chinese Academy of Sciences (XDB27030103) and the Chinese Academy of Sciences.

References

Aida, M., Beis, D., Heidstra, R., Willemsen, V., Blilou, I., Galinha, C., Nussaume, L., Noh, Y.-S., Amasino, R. and Scheres, B. (2004). The PLETHORA genes mediate patterning of the Arabidopsis root stem cell niche. *Cell* **119**, 109-120. doi:10.1016/j.cell.2004.09.018

Atta, R., Laurens, L., Boucheron-Dubuisson, E., Guivarc'h, A., Carnero, E., Giraudat-Pautot, V., Rech, P. and Chriqui, D. (2009). Pluripotency of Arabidopsis xylem pericycle underlies shoot regeneration from root and hypocotyl explants grown in vitro. *Plant J.* **57**, 626-644. doi:10.1111/j.1365-313X.2008.03715.x

Che, P., Lall, S. and Howell, S. H. (2007). Developmental steps in acquiring competence for shoot development in Arabidopsis tissue culture. *Planta* **226**, 1183-1194. doi:10.1007/s00425-007-0565-4

Cools, T., Iantcheva, A., Maes, S., Van den Daele, H. and De Veylder, L. (2010). A replication stress-induced synchronization method for Arabidopsis thaliana root meristems. *Plant J.* **64**, 705-714. doi:10.1111/j.1365-313X.2010.04361.x

De Los Angeles, A., Ferrari, F., Xi, R., Fujiwara, Y., Benvenisty, N., Deng, H., Hochedlinger, K., Jaenisch, R., Lee, S., Leitch, H. G. et al. (2015). Hallmarks of pluripotency. *Nature* **525**:469-478. doi:10.1038/nature15515

Di Laurenzio, L., Wysocka-Diller, J., Malamy, J. E., Pysh, L., Helariutta, Y., Freshour, G., Hahn, M. G., Feldmann, K. A. and Benfey, P. N. (1996). The SCARECROW gene regulates an asymmetric cell division that is essential for generating the radial organization of the Arabidopsis root. *Cell* **86**, 423-433. doi:10.1016/S0092-8674(00)80115-4

Duclercq, J., Sangwan-Norreel, B., Catterou, M. and Sangwan, R. S. (2011). De novo shoot organogenesis: from art to science. *Trends Plant Sci.* **16**, 597-606. doi:10.1016/j.tplants.2011.08.004

Fan, M., Xu, C., Xu, K. and Hu, Y. (2012). LATERAL ORGAN BOUNDARIES DOMAIN transcription factors direct callus formation in Arabidopsis regeneration. *Cell Res.* **22**, 1169-1180. doi:10.1038/cr.2012.63

Gallagher, K. L., Paquette, A. J., Nakajima, K. and Benfey, P. N. (2004). Mechanisms regulating SHORT-ROOT intercellular movement. *Curr. Biol* **14**, 1847-1851. doi:10.1016/j.cub.2004.09.081

Gordon, S. P., Heisler, M. G., Reddy, G. V., Ohno, C., Das, P. and Meyerowitz, E. M. (2007). Pattern formation during de novo assembly of the Arabidopsis shoot meristem. *Development* **134**, 3539-3548. doi:10.1242/dev.010298

Gordon, S. P., Chickarmane, V. S., Ohno, C. and Meyerowitz, E. M. (2009). Multiple feedback loops through cytokinin signaling control stem cell number within the Arabidopsis shoot meristem. *Proc. Natl. Acad. Sci. USA* **106**, 16529-16534. doi:10.1073/pnas.0908122106

He, C., Chen, X., Huang, H. and Xu, L. (2012). Reprogramming of H3K27me3 is critical for acquisition of pluripotency from cultured Arabidopsis tissues. *PLoS Genet.* **8**, e1002911. doi:10.1371/journal.pgen.1002911

Helariutta, Y., Fukaki, H., Wysocka-Diller, J., Nakajima, K., Jung, J., Sena, G., Hauser, M.-T. and Benfey, P. N. (2000). The SHORT-ROOT gene controls radial patterning of the Arabidopsis root through radial signaling. *Cell* **101**, 555-567. doi:10.1016/S0092-8674(00)80865-X

Hiratsu, K., Matsui, K., Koyama, T. and Ohme-Takagi, M. (2003). Dominant repression of target genes by chimeric repressors that include the EAR motif, a repression domain, in Arabidopsis. *Plant J.* **34**, 733-739. doi:10.1046/j.1365-313X.2003.01759.x

Hu, X. and Xu, L. (2016). Transcription factors WOX11/12 directly activate WOX5/7 to promote root primordia initiation and organogenesis. *Plant Physiol.* **172**, 2363-2373. doi:10.1104/pp.16.01067

Hu, B., Zhang, G., Liu, W., Shi, J., Wang, H., Qi, M., Li, J., Qin, P., Ruan, Y., Huang, H. et al. (2017). Divergent regeneration-competent cells adopt a common mechanism for callus initiation in angiosperms. *Regeneration* **4**, 132-139. doi:10.1002/reg2.82

Ikeuchi, M., Favero, D. S., Sakamoto, Y., Iwase, A., Coleman, D., Rymen, B. and Sugimoto, K. (2019). Molecular mechanisms of plant regeneration. *Annu. Rev. Plant Biol.* **70**, 377-406. doi:10.1146/annurev-arplant-050718-100434

Ishihara, H., Sugimoto, K., Tarr, P. T., Temman, H., Kadokura, S., Inui, Y., Sakamoto, T., Sasaki, T., Aida, M., Suzuki, T. et al. (2019). Primed histone demethylation regulates shoot regenerative competency. *Nat. Commun.* **10**, 1786. doi:10.1038/s41467-019-09386-5

Kareem, A., Durgaprasad, K., Sugimoto, K., Du, Y., Pulianmackal, A. J., Trivedi, Z. B., Abhayadev, P. V., Pinon, V., Meyerowitz, E. M., Scheres, B. et al. (2015). PLETHORA genes control regeneration by a two-step mechanism. *Curr. Biol.* **25**:1017-1030. doi:10.1016/j.cub.2015.02.022

Kim, J.-Y., Yang, W., Forner, J., Lohmann, J. U., Noh, B. and Noh, Y.-S. (2018). Epigenetic reprogramming by histone acetyltransferase HAG1/AtGCN5 is required for pluripotency acquisition in Arabidopsis. *EMBO J.* **37**, e98726. doi:10.15252/embj.201798726

Kubo, M., Udagawa, M., Nishikubo, N., Horiguchi, G., Yamaguchi, M., Ito, J., Mimura, T., Fukuda, H. and Demura, T. (2005). Transcription switches for protoxylem and metaxylem vessel formation. *Genes Dev.* **19**, 1855-1860. doi:10.1101/gad.1331305

Kurihara, D., Mizuta, Y., Sato, Y. and Higashiyama, T. (2015). ClearSee: a rapid optical clearing reagent for whole-plant fluorescence imaging. *Dev* **142**, 4168-4179. doi:10.1242/dev.127613

Lee, K., Park, O.-S. and Seo, P. J. (2018). JMJ30-mediated demethylation of H3K9me3 drives tissue identity changes to promote callus formation in Arabidopsis. *Plant J.* **95**, 961-975. doi:10.1111/tpj.14002

Lee, K., Park, O.-S., Choi, C. Y. and Seo, P. J. (2019a). ARABIDOPSIS TRITHORAX 4 facilitates shoot identity establishment during the plant regeneration process. *Plant Cell Physiol.* **60**, 826-834. doi:10.1093/pcp/pcy248

Lee, K.-H., Du, Q., Zhuo, C., Qi, L. and Wang, H. (2019b). LBD29-involved auxin signaling represses NAC master regulators and fiber wall biosynthesis. *Plant Physiol.* **181**, 595-608. doi:10.1104/pp.19.00148

Lee, K., Park, O.-S., Go, J. Y., Yu, J., Han, J. H., Kim, J., Bae, S., Jung, Y. J. and Seo, P. J. (2021). Arabidopsis ATXR2 represses de novo shoot organogenesis in the transition from callus to shoot formation. *Cell Rep.* **37**, 109980. doi:10.1016/j.celrep.2021.109980

Liu, J., Sheng, L., Xu, Y., Li, J., Yang, Z., Huang, H. and Xu, L. (2014). WOX11 and 12 are involved in the first-step cell fate transition during de novo root organogenesis in Arabidopsis. *Plant Cell* **26**, 1081-1093. doi:10.1105/tpc.114.122887

Liu, J., Hu, X., Qin, P., Prasad, K., Hu, Y. and Xu, L. (2018). The WOX11-LBD16 pathway promotes pluripotency acquisition in callus cells during de novo shoot regeneration in tissue culture. *Plant Cell Physiol.* **59**, 734-743. doi:10.1093/pcp/pcy010

Mähönen, A. P., Bonke, M., Kauppinen, L., Riikonen, M., Benfey, P. N. and Helariutta, Y. (2000). A novel two-component hybrid molecule regulates vascular morphogenesis of the Arabidopsis root. *Genes Dev.* **14**, 2938-2943. doi:10.1101/gad.189200

Marquès-Bueno, M. M., Morao, A. K., Cayrel, A., Platre, M. P., Barberon, M., Caillieux, E., Colot, V., Jaillais, Y., Roudier, F. and Vert, G. (2016). A versatile Multisite Gateway-compatible promoter and transgenic line collection for cell type-specific functional genomics in Arabidopsis. *Plant J.* **85**, 320-333. doi:10.1111/tpj.13099

Motte, H., Vereecke, D., Geelen, D. and Werbrouck, S. (2014). The molecular path to in vitro shoot regeneration. *Biotechnol. Adv* **32**, 107-121. doi:10.1016/j.biotechadv.2013.12.002

Nakajima, K., Sena, G., Nawy, T. and Benfey, P. N. (2001). Intercellular movement of the putative transcription factor SHR in root patterning. *Nature* **413**, 307-311. doi:10.1038/35095061

Okushima, Y., Fukaki, H., Onoda, M., Theologis, A. and Tasaka, M. (2007). ARF7 and ARF19 regulate lateral root formation via direct activation of LBD/ASL genes in Arabidopsis. *Plant Cell* **19**, 118-130. doi:10.1105/tpc.106.047761

Robinton, D. A. and Daley, G. Q. (2012). The promise of induced pluripotent stem cells in research and therapy. *Nature* **481**, 295-305. doi:10.1038/nature10761

Sabatini, S., Heidstra, R., Wildwater, M. and Scheres, B. (2003). SCARECROW is involved in positioning the stem cell niche in the Arabidopsis root meristem. *Genes Dev.* **17**, 354-358. doi:10.1101/gad.252503

Sang, Y. L., Cheng, Z. J. and Zhang, X. S. (2018). iPSCs: a comparison between animals and plants. *Trends Plant Sci.* **23**, 660-666. doi:10.1016/j.tplants.2018.05.008

Santuari, L., Sanchez-Perez, G. F., Luijten, M., Rutjens, B., Terpstra, I., Berke, L., Gorte, M., Prasad, K., Bao, D., Timmermans-Hereijgers, J. L. P. M. et al. (2016). The PLETHORA gene regulatory network guides growth and cell differentiation in Arabidopsis roots. *Plant Cell* **28**:2937-2951. doi:10.1105/tpc.16.00656

Sheng, L., Hu, X., Du, Y., Zhang, G., Huang, H., Scheres, B. and Xu, L. (2017). Non-canonical WOX11-mediated root branching contributes to plasticity in Arabidopsis root system architecture. *Development* **144**, 3126-3133. doi:10.1242/dev.152132

Shimotohno, A., Heidstra, R., Blilou, I. and Scheres, B. (2018). Root stem cell niche organizer specification by molecular convergence of PLETHORA and SCARECROW transcription factor modules. *Genes Dev.* **32**, 1085-1100. doi:10.1101/gad.314096.118

Skoog, F. and Miller, C. O. (1957). Chemical regulation of growth and organ formation in plant tissues cultured in vitro. *Symp. Soc. Exp. Biol* **11**, 118-130.

Sugimoto, K., Jiao, Y. and Meyerowitz, E. M. (2010). Arabidopsis regeneration from multiple tissues occurs via a root development pathway. *Dev. Cell* **18**, 463-471. doi:10.1016/j.devcel.2010.02.004

Sugimoto, K., Gordon, S. P. and Meyerowitz, E. M. (2011). Regeneration in plants and animals: dedifferentiation, transdifferentiation, or just differentiation? *Trends Cell Biol.* **21**, 212-218. doi:10.1016/j.tcb.2010.12.004

Welch, D., Hassan, H., Blilou, I., Immink, R., Heidstra, R. and Scheres, B. (2007). Arabidopsis JACKDAW and MAGPIE zinc finger proteins delimit asymmetric cell division and stabilize tissue boundaries by restricting SHORT-ROOT action. *Genes Dev.* **21**, 2196-2204. doi:10.1101/gad.440307

Wu, S., Lee, C.-M., Hayashi, T., Price, S., Divol, F., Henry, S., Pauluzzi, G., Perin, C. and Gallagher, K. L. (2014). A plausible mechanism, based upon SHORT-ROOT movement, for regulating the number of cortex cell layers in roots. *Proc. Natl. Acad. Sci. USA* **111**, 16184-16189. doi:10.1073/pnas.1407371111

Wu, L.-Y., Shang, G.-D., Wang, F.-X., Gao, J., Wan, M.-C., Xu, Z.-G. and Wang, J.-W. (2022). Dynamic chromatin state profiling reveals regulatory roles of auxin and cytokinin in shoot regeneration. *Dev. Cell* **57**, 526-542.e7. doi:10.1016/j.devcel.2021.12.019

Xu, L. (2018). De novo root regeneration from leaf explants: wounding, auxin, and cell fate transition. *Curr. Opin. Plant Biol* **41**, 39-45. doi:10.1016/j.pbi.2017.08.004

Yin, K., Ueda, M., Takagi, H., Kajihara, T., Sugamata Aki, S., Nobusawa, T., Umeda-Hara, C. and Umeda, M. (2014). A dual-color marker system for in vivo visualization of cell cycle progression in Arabidopsis. *Plant J.* **80**, 541-552. doi:10.1111/tpj.12652

Zhai, N. and Xu, L. (2021). Pluripotency acquisition in the middle cell layer of callus is required for organ regeneration. *Nat. Plants* **7**, 1453-1460. doi:10.1038/s41477-021-01015-8

Zhang, G., Zhao, F., Chen, L., Pan, Y., Sun, L., Bao, N., Zhang, T., Cui, C.-X., Qiu, Z., Zhang, Y. et al. (2019). Jasmonate-mediated wound signalling promotes plant regeneration. *Nat. Plants* **5**:491-497. doi:10.1038/s41477-019-0408-x

Zuo, J., Niu, Q.-W. and Chua, N.-H. (2000). Technical advance: An estrogen receptor-based transactivator XVE mediates highly inducible gene expression in transgenic plants. *Plant J.* **24**, 265-273. doi:10.1046/j.1365-313x.2000.00868.x